ISSN: 2277-3754
ISO 9001:2008 Certified
International Journal of Engineering and Innovative Technology (IJEIT)
Volume 3, Issue 3, September 2013

Lateral Jet Interaction with the External Flow Field Features on Re-entry Vehicle

S.Srinivas Prasad[1], K.Durga Rao[2], R.K.Sharma[3], G.V.Ramana Murty[4]
[1]Professor, Department of Aeronautical Engineering, MLR Institute of Technology, Hyderabad
sanakaprasad@yahoo.com
[2]Associate professor, Department of Aeronautical Engineering, Malla Reddy College of Engineering and Technology, Hyderabad
durgaraok9@gmail.com
[3]Scientist G, DRDL, Hyderabad, India
dr_rk_sharma@yahoo.com
[4]Professor, Department of Mechanical Engineering, Vasavi college of Engineering, Hyderabad
ramanamurty.govindaraju@gmail.com

Abstract- ***Numerical investigation of the interaction between a lateral jet and external flow has been performed on a re-entry vehicle. The geometry used for the analysis is a typical re-entry vehicle employed aft jet for its control. The flow structure of lateral jets issuing in to hypersonic cross flow at 8.1 Mach number, at $\alpha = 5^0$ is examined. A circular air jet injected at right angles to the body surface from leeward side of a re-entry vehicle. Three dimensional Navier-Stokes equations along with k-ω SST turbulence model are solved using commercial CFD software. As the jet was turned downstream by the external flow forms a barrel shock.***

Index Terms- **Aerodynamics, CFD, Hypersonic Flow, Reentry vehicle.**

NOMENCLATURE

α	=	Angle of attack
M_∞	=	Mach number
JPR	=	Jet pressure ratio
p	=	Static Pressure
T	=	Temperature
p_∞	=	Free stream Pressure
d	=	Reference diameter

I. INTRODUCTION

Missiles/Re-entry vehicles need some kind of a control mechanism for maneuvering. Changing the trajectory of a missile is done by imposing additional aerodynamic forces on the missile. Conventional control systems consist of deflecting lifting surfaces located on the body of the missile. This type of control is also called aerodynamic control. Canard control type and tail control type are two most common types used for aerodynamic control. Deflection of these control surfaces is done by actuating systems. These systems consist of electric/ pneumatic/ hydraulic motors and control input is given by the autopilot or manually, depending on the subsystem of the missile. Other than control surface deflection, reaction type control systems have recently been used in the missiles. In this type, instead of a deflecting lifting surface, high speed ejecting fluid or thrust deflection techniques are used to create a maneuvering force. Reentry vehicles often do not have aerodynamic control surfaces. Even reentry vehicle employed aerodynamic surfaces for control during reentry, will be ineffective because of very low dynamic pressure at higher altitude. Therefore, the reaction control system is still important to control the vehicle. At higher altitudes, lateral jets offer the only possibility to exert sufficient control forces for reentry vehicle. High pressure jets are ejected into free stream in normal direction and they create forces and moments for maneuvering. These control systems can be seen[1] schematically in Fig 1.

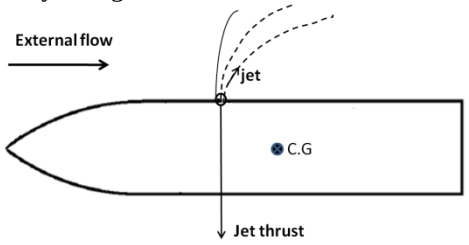

Fig 1 Lateral jet injected into external flow

The ejection of jet in upward direction causes a downward force from the fluid to the projectile and this force creates pitching moment about centre of gravity for manoeuvring. Interaction of the jet with the free stream results in a highly complicated flow field[2]. It is characterized by shock/shock interactions and shock/ boundary layer interactions. Currently, inadequate information is available on jet interaction flow field developed between the lateral jet and external flow over re-entry vehicle. Lateral jet controls systems are being considered as attractive alternatives to conventional surface control systems in recent years[3]. There are some advantages of these systems to conventional control surfaces. In low dynamic pressures, at high altitude or low speed flight, conventional control surfaces lose their control effectiveness. Lateral jet control systems are highly effective in high altitude, low density regions. The lateral jet control has quick control for a re-entry vehicle and is effective to make corrections for the disturbances encountered during ascent and descent phase in the trajectory. Conventional control systems always contain a larger lag in control input and system response than reaction type control systems.

ISSN: 2277-3754
ISO 9001:2008 Certified
International Journal of Engineering and Innovative Technology (IJEIT)
Volume 3, Issue 3, September 2013

Missiles with conventional control surfaces have stall problem at high angles of attack. Stalling results in flow separation and loss of control effectiveness for lifting surfaces[4]. Thus control surface deflection angle and angle of attack for the projectile are limited to some extent. But lateral jet controlled missiles/ re-entry vehicles do not have a stall problem so that they can provide higher angles of attack to the missile. The aim of present paper is to clearly identify the complex flow physics resulting from the interaction of hypersonic free stream with lateral jet.

II. BODY GEOMETRY CONSIDERED IN THE PRESENT INVESTIGATION

The reentry configuration used in the present study is a spherically blunted cone having 10.3^0 semi apex angle with a bluntness ratio of 0.523. The lateral jet is turned off and the jet is considered as a wall. This condition is called jet-off condition in the present study. The body geometry used and the direction of normal and axial forces are shown in Fig 1. The diameter of the lateral jet is 2 mm and is at a distance of 0.33d from base on leeward side.

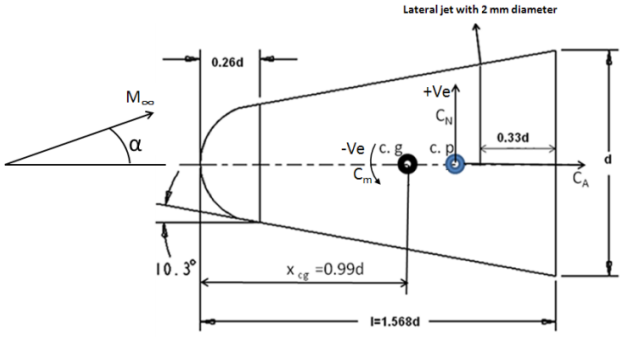

Fig 2 Schematic view of model with sign convection used for normal force and pitching moment

III. GRID GENERATION

The geometry and structured mesh were created using the grid generation software Gambit 2.4.6 supplied in FLUENT software suite. A parabolic computational domain is created around the reentry body. Computational domain has been considered such that the outer boundary does not interfere with the jet flow.

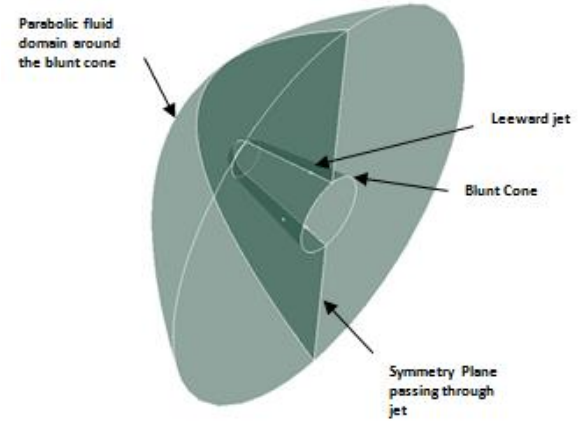

Fig 3 Fluid domain around Vehicle

The physical domain under consideration is shown in Fig 3 which consists of the reentry body and fluid domain. Hexahedral cells are used in the entire domain. Grid points were concentrated more near the jet exit in order to resolve the larger gradient in flow variables. In generating the mesh, boundary layer mesh spacing was used near the reentry body surface. Fine mesh is used near the jet and growth rate has been maintained away from the body.

IV. GOVERNING EQUATIONS OF FLUID FLOW

The CFD code models the conservation equations of mass, momentum and energy in terms of the dependent variables (Velocity, pressure and enthalpy). They are time dependent in a turbulent flow. These quantities are decomposed into a mean component and a fluctuating one and the original conservation equations are converted to an averaged form. For compressible flows, the mean form of equations is obtained through a time-averaging process, usually called Reynolds stress averaging and a technique of mass averaging, also called Favre averaging. The original equations for the conservations of mass, momentum and energy are expressed in terms of time and Favre averaged quantities.

The momentum and energy equations contain terms that cannot be expressed as function of the mean flow variables which are the Reynolds stresses, the turbulent energy fluxes and the fluctuating viscous work term. These terms are related to known quantities by using a turbulence model before a close solution of the equations becomes possible.

The governing equations of a compressible turbulent flow can be written using time-averaged (Reynolds-averaged, indicated by an overbar) values of the density, pressure and mass- weighted (Favre-averaged, indicated by a tilde) averages for the Velocity components and Temperature. Prime indicates the fluctuating component coming from the mass-averaged process. Double prime indicates the fluctuating component coming from the mass averaged process.

The governing equations used in this study are presented in their differential form.

Conservation of mass,

$$\frac{\partial \bar{\rho}}{\partial t} + \frac{\partial (\bar{\rho}\tilde{u}_j)}{\partial x_j} = 0 \qquad \text{Eq. 1}$$

Conservation of momentum

$$\frac{\partial \bar{\rho}\tilde{u}_i}{\partial t} + \frac{\partial (\bar{\rho}\tilde{u}_j\tilde{u}_i)}{\partial x_j} = -\frac{\partial \bar{p}}{\partial x_i} + \frac{\partial}{\partial x_j}\left[\mu\left(\frac{\partial \tilde{u}_i}{\partial x_j} + \frac{\partial u_j}{\partial x_i} - \frac{2}{3}\delta_{ij}\frac{\partial \tilde{u}_l}{\partial x_l}\right)\right] + \frac{\partial}{\partial x_j}\left(-\bar{\rho}\,\widetilde{u''_i u''_j}\right) \qquad \text{Eq. 2}$$

The above equation contains term that cannot be expressed as a function of the mean flow variables. This term is called Reynolds stress tensor defined by $(-\bar{\rho}\,\widetilde{u''_i u''_j})$. Boussinesq hypothesis is used to relate the Reynolds stresses to the mean velocity gradients. The advantage of this approach is the relatively low computational cost associated with the computation of the turbulent viscosity (μ_t).

$$-\bar{\rho}\,\widetilde{u''_i u''_j} = \mu_t\left(\frac{\partial \tilde{u}_i}{\partial x_j} + \frac{\partial u_j}{\partial x_i}\right) - \frac{2}{3}\delta_{ij}\left(\rho k + \mu_t \frac{\partial u_k}{\partial x_k}\right) \qquad \text{Eq. 3}$$

Conservation of energy,

ISSN: 2277-3754
ISO 9001:2008 Certified
International Journal of Engineering and Innovative Technology (IJEIT)
Volume 3, Issue 3, September 2013

$$\frac{\partial \bar{\rho} e_0}{\partial t} + \frac{\partial(\bar{\rho} e_0 \tilde{u}_j + \bar{p}\tilde{u}_j + \bar{\rho}\widetilde{e''_0 u''_j})}{\partial x_j} = \frac{\partial[(-\bar{p}\delta_{ij} + \bar{\tau}_{ij})\tilde{u}_i]}{\partial x_j} - \frac{\partial(\overline{q_t})}{\partial x_j} \quad \text{Eq. 4}$$

Where $e_0 = \overline{C_v T} + \frac{1}{2}\tilde{u}_j \tilde{u}_j + \frac{1}{2}\widetilde{u''_j u''_j}$ Eq. 5

SST k-ω Turbulence Model

The shear stress transport k-ω model is the only variation of the standard k-ω model available in FLUENT. It was developed by Menter (1994) using the standard k-ω model and a transformed k-epsilon model. The main difference is the way in which the model calculates the turbulent viscosity to account for the transport of the principal turbulent shear stress. This model also incorporates a cross-diffusion term in the ω equation and a blending function to allow proper calculation of the near-wall and far-field areas. The blending function triggers the standard k-ω model in near wall regions and triggers the k-ε like model in areas away from the surface. These differences make the SST model more precise for a larger variety of flows than the standard model.

Similar to the standard k-ω model, the transport equations for k and ω are slightly modified and are given by

$$\frac{\partial(\rho k)}{\partial t} + \frac{\partial(\rho k u_i)}{\partial x_i} = \frac{\partial}{\partial x_j}\left[(\mu + \frac{\mu_t}{\sigma_k})\frac{\partial k}{\partial x_j}\right] + \widetilde{G_k} - Y_k + S_k \quad \text{Eq. 6}$$

$$\frac{\partial(\rho\omega)}{\partial t} + \frac{\partial(\rho\omega u_i)}{\partial x_i} = \frac{\partial}{\partial x_j}\left[(\mu + \frac{\mu_t}{\sigma_\omega})\frac{\partial k}{\partial x_j}\right] + G_\omega - Y_\omega + D_\omega + S_\omega \quad \text{Eq. 7}$$

Where $\widetilde{G_k}$ represents the generation of turbulent kinetic energy arises due to mean velocity gradients, G_ω is generation of ω and Y_k and Y_ω represent the dissipation of k and ω due to turbulence. α_k and α_ω are the turbulent Prandt1 numbers for k and ω respectively and S_ε and S_k are source terms defined by the user. D_ω is the cross-diffusion term.

V. Flow Solver Description

Commercial CFD software FLUENT is used for the simulation. The simulation has been performed with an implicit compressible flow solver. The flow field is assumed to be compressible and turbulent. CFD studies are carried out to determine the flow and aerodynamic coefficients on the selected reentry configuration. The implicit, compressible (coupled) solver was used. The shear stress transport k-omega two equation model was used for the flow variables and the turbulent viscosity equation. The initial conditions were set to the previously defined free stream conditions and are applicable to all simulations in this study.

VI. Boundary Conditions

A far-field boundary condition is used in FLUENT to model a free stream condition at inlet to domain with free stream Mach number at $\alpha = 5^0$ and static conditions. The Mach number ($M_\infty = 8.1$), the static temperature ($T\infty = 267.3$ K) and the static pressure ($P\infty = 550$ Pa) are used for external flow simulation. Turbulent viscosity is defined as 1% of the free stream at inlet. Mass flow boundary condition is used to provide a prescribed jet mass flow rate or mass flux distribution at a jet inlet. Mass flow rate at the jet exit is 0.068 kg/s and the jet pressure is 0.64 MPa. Pressure outlet boundary condition is used to define the static pressure at domain outlet. The re-entry vehicle body wall was modeled as no-slip condition. Iterative procedure requires that all solution variables be initialized before calculating a solution. Initialize the entire flow field using the values set for far-field in the present study. A symmetry boundary condition applies to the symmetry plane of the problem.

VII. Results and Discussion

Simulations have been carried out on a typical re-entry vehicle in order to understand the effect of a lateral jet interaction with the external flow for the operating conditions specified in Table1. The computed results have been presented with jet-off and jet-on conditions in the present study. Main features of lateral jet interaction flow field are presented in contours, vectors and streamlines indicated by magnitude of Mach number.

A Mach contours for jet-off condition are shown in Fig 4(a) represent the base flow pattern on re-entry configuration in pitch plane. A detached shock wave stands in front of the body. Asymmetry in shock wave is because of angle of attack ($\alpha = 5^0$). The Mach contours for jet-on condition are illustrated in Fig 4(b). Significant changes in the flow field are observed due to jet interaction near the region of lateral jet. The dominant features of the jet interaction between the lateral jet and the external flow are illustrated in Fig 5 with a zoomed view of Fig 4(b) near the lateral jet. A detailed flow field topology in the pitch plane near the lateral jet region is indicated.

Table 1 Operating conditions used for simulation

JPR	α Degrees	Altitude (km)	Jet mass flow rate (kg/s)	Location of jet	Mach number
1100	5	35	0.068	leeward side	8.1

The under expanded jet emerged from the nozzle obstructed the free stream approaching from left. The obstruction deflected the free stream in the transverse and lateral directions generating a three dimensional shock wave referred as jet bow shock. As the jet was turned, an oblique shock wave formed within jet, typically referred as a barrel shock. The lateral jet expands through Prandtl-Meyer fan at the lip of the orifice into the jet plume which is enclosed in a barrel shock and Mach disk. The Mach disk is essentially a normal shock that slows down the high speed flow inside the plume to relatively low speed flow. The low speed flow that is generated by the Mach disk forms a lip surface with the supersonic fluid flowing around and past the barrel shock. The slip surface is indicated by a line in the Mach contours. The bow shock interacted with the approaching boundary layer to create shock/boundary layer interaction region. The pressure gradient across the bow shock induces separation of

ISSN: 2277-3754
ISO 9001:2008 Certified
International Journal of Engineering and Innovative Technology (IJEIT)
Volume 3, Issue 3, September 2013

the incoming boundary layer which in turn creates a separation shock. A separation zone develops upstream from the jet due to boundary layer separation. The low pressure region behind the jet was found to be created by the reflection of the barrel shock.

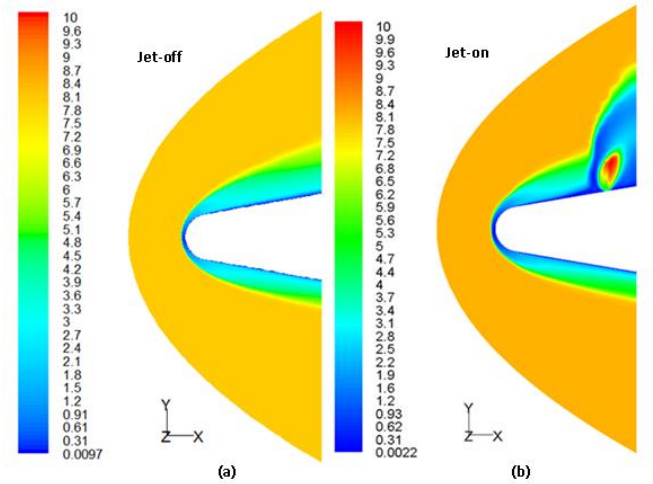

Fig 4 Mach Contours with jet-off and jet-on at $\alpha = 5^0$, $M_\infty = 8.1$

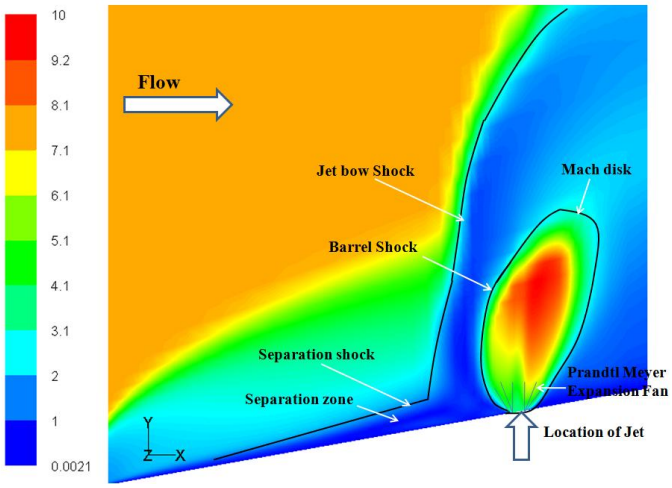

Fig 5 Jet interaction flow field Mach contours

The flow near the location of jet with jet-off condition is shown in Fig 6. The velocity vectors with jet-off condition are smooth and flow follows the body geometry. The flow field developed due to jet interaction is represented with velocity vectors near the jet region in pitch plane as shown in Fig 7. The stream lines near the jet are smooth over the vehicle for jet-off condition as shown in Fig 8. The jet interaction flow field near the jet region for jet-on case is as shown in Fig 9. The direction of the external flow and the lateral jet are represented. The recirculation zone ahead of the jet is clearly seen due to separation shock. The separation line and the bow shock are also observed from the stream lines colored by velocity. The change in the direction of the jet in the downstream direction by the free stream is represented near the jet. The streamlines on the vehicle with jet-off condition are smooth and follow the vehicle as shown in Fig 10. For jet-on case, the stream lines do not follow the body. The lateral jet acts as an obstacle to the external flow and the flow is diverted by the external flow in the jet interaction region as shown in Fig 11.

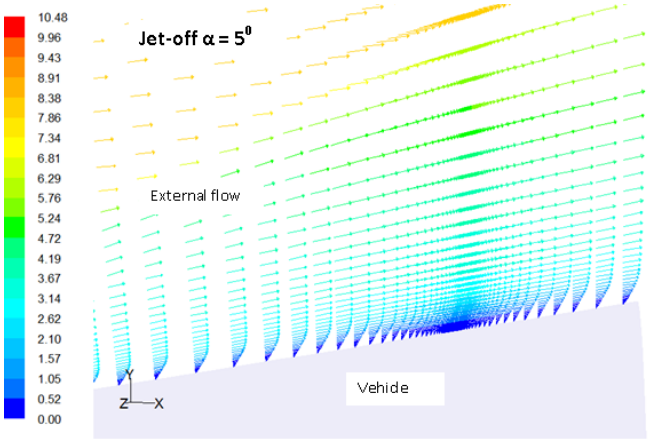

Fig 6 Velocity vectors colored by Mach number for jet-off condition

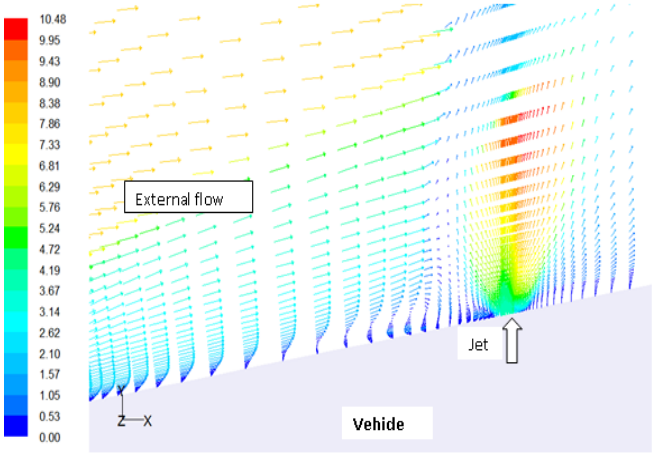

Fig 7 Velocity vectors colored by Mach number near the jet interaction region at $\alpha = 5^0$

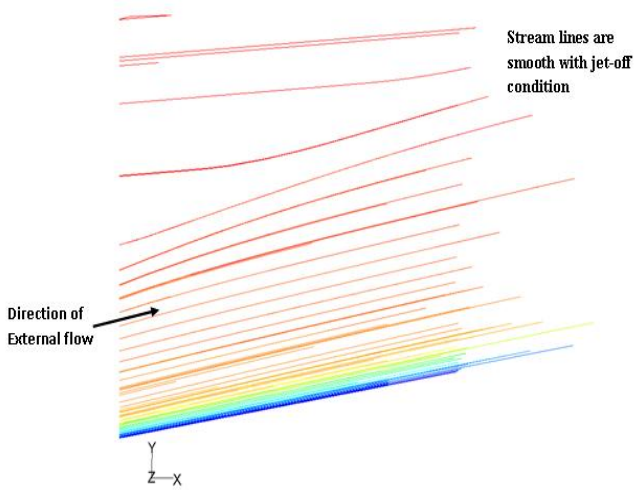

Fig 8 Zoomed view of stream lines in the jet region for jet-off condition

ISSN: 2277-3754
ISO 9001:2008 Certified
International Journal of Engineering and Innovative Technology (IJEIT)
Volume 3, Issue 3, September 2013

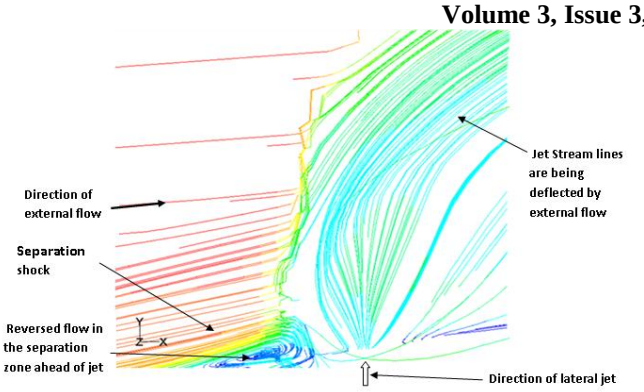

Fig 9 Zoomed view of stream lines in the jet interaction region

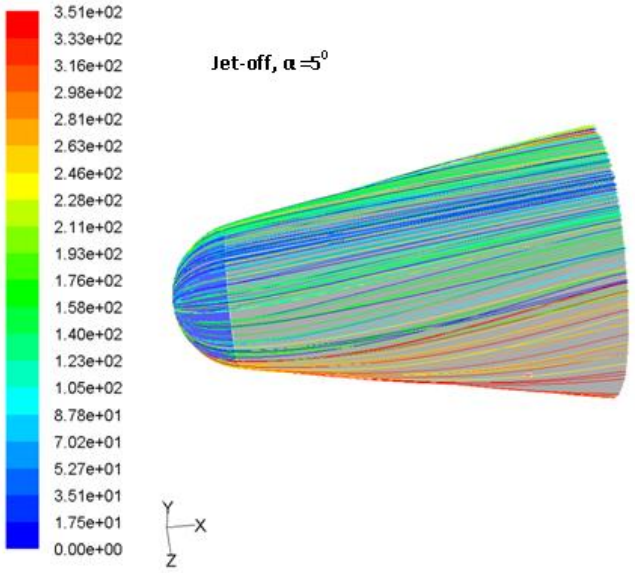

Fig 10 Jet-off external flow stream lines over the body

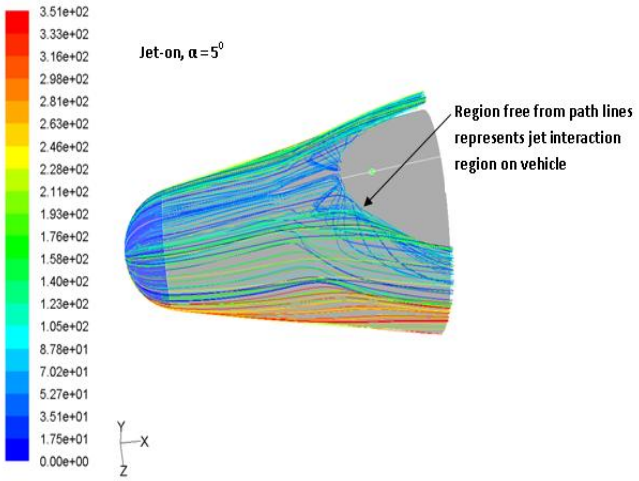

Fig 11 Jet-on external flow stream lines over the body near the jet region

The normal force coefficient, pitching moment coefficient values are found from numerical solution by taking the base area as reference area. The ratio of the normal force coefficient to pitching moment coefficient gives the location of non dimensional centre of pressure value. These values are given in Table 2.

Table 2 Comparison of C_N and C_m at $M_\infty = 8.1$, $\alpha = 5^0$

α	Jet Location	C_N	C_m	X_{cp}/d
5	Jet off	0.114	-0.098	0.859
5	Jet on	0.062	-0.051	0.822

VIII. CONCLUSION

The velocity vectors, Mach Contours and streamlines presented in this section around the re-entry vehicle allow a detailed exploration of the complex flow field created by the jet interaction with the external flow. The comparison of jet-on results with jet-off reveals that the flow structure is altered by the jet interaction around the jet. The force and moment generated by the jet interaction phenomenon augments the control force and moment produced by lateral jet. Normal force coefficient is reduced by 45.6% due to jet interaction. Pitching moment coefficient is reduced by 48% due to jet interaction. The centre of pressure shifts forward by 0.06d. This indicates that the aerodynamic stability of vehicle reduces due lateral jet interaction. Even a small jet of 2mm, produces significant aerodynamic forces on hypersonic re-entry body which can be applied to control the vehicle orientation.

REFERENCES

[1] Fleeman, E., L, "Tactical Missile Design", AIAA Education Series, 2001.

[2] Cassel, L., A., "Applying Jet Interaction Technology", AIAA Journal of Spacecraft and Rockets, Vol.40, No.4, 2003, pp.523-637.

[3] Srivastava.B .B "Computational analysis and validation for lateral jet controlled Missiles "Journal of space craft and rockets" Vol.34, No.5, September-October 1997.

[4] Anderson, J., D., "Fundamentals of Aerodynamics", McGraw and Hill, 2001.

[5] Champigny, P, and Lacau. R. G, "Lateral jet Control for tactical Missiles," Special course on missile aerodynamics, AGARD-FDP Von Karman Institute, Brussels, Belgium, 6-10 June 1994, pp. 3.1-3.57.

[6] Srinivas Prasad S, "Investigation of lateral jet interaction with the external flow on a re-entry vehicle" PhD thesis, Osmania University, Hyderabad June 2013.

[7] Srinivas Prasad.S, R.K.Sharma, G.V.Ramana Murthy, K.Durga Rao "Effect of lateral jet interaction with external flow at positive and negative incidence" International Journal of Engineering and Innovative Technology, Volume 2, issue 12, July 2013.

[8] Kurita.M, Tsuyoshi Inoue and Nakamura.Y "Aerodynamic interaction due to side jet from a blunted cone in hypersonic flow"AIAA-2000-4518.

[9] Kurita.M, Okada .T and Nakamura.Y "The Effects of attack angle on aerodynamic interaction due to side jet from a blunted body in a supersonic flow" AIAA 2001-0261.

[10] Kurita.M, Okada .T and Nakamura.Y" The Effects of attack angle on side jet aerodynamic interaction in blunted body at hypersonic flow."AIAA 2001-1825.

ISSN: 2277-3754
ISO 9001:2008 Certified
International Journal of Engineering and Innovative Technology (IJEIT)
Volume 3, Issue 3, September 2013

[11] Kennedy .K, Walker. B and Mikkelson.C "Jet interaction effects on a missile with aerodynamic control surfaces" AIAA Paper 99-0807, January 1999.

[12] Gimelshein S.F, Alexeenko A.A. and Levin D.A. "Modeling of the interaction of a side jet with a rarefied atmosphere "Journal of spacecraft and rockets "Vol.39, No.2, March-April 2002.

[13] Tetsuya Nakamura, Munetsugu Kaneko, Igor Menshov and Yoshiaki Nakamura" Numerical simulation on aerodynamic interaction between a side jet and flow around a blunt body in hypersonic flow" AIAA - 2003-1135.

[14] Valerio Viti Joseph Schetz and Reece Neel" Comparison of first and second Order turbulence models for a Jet/3D ramp combination in supersonic flow" AIAA 2005-1100.

AUTHOR BIOGRAPHY

Srinivas Prasad S got PhD from Osmania University Hyderabad under the guidance of Dr.R.K.Sharma and Dr.G.V.Ramana murty. Working as a Professor and Head in Department of Aeronautical Engineering, MLR Institute of Technology, Hyderabad. Areas of interests are Aerodynamics, Turbo machinery, Propulsion.

K.Durga Rao is pursuing PhD from JNTU Hyderabad. He is working as an Associate Professor in Department of Aeronautical Engineering, Mallareddy college of Engineering and Technology Hyderabad.

Dr.R.K.Sharma, Scientist G and Project director HSTDV, DRDL Hyderabad.

Dr. G.V Ramana murty former General manager BHEL R&D Hyderabad and currently working as a Professor and Head Department of Mechanical Engineering, Vasavi College of Engineering. His areas of interests are Turbo machinery, Gas dynamics.